



Constraints on Lorentz invariance violation from GRB 221009A using the DisCan method*

Yu Xi (习余)^{1,2}  Fu-Wen Shu (舒富文)^{1,2,3†} 

¹Department of Physics, Nanchang University, Nanchang 330031, China

²Center for Relativistic Astrophysics and High Energy Physics, Nanchang University, Nanchang 330031, China

³Center for Gravitation and Cosmology, Yangzhou University, Yangzhou 225009, China

Abstract: Lorentz symmetry is a cornerstone of modern physics, and testing its validity remains a critical endeavor. In this study, we analyze the photon time-of-flight and time-shift data from LHAASO observations of Gamma-Ray Burst GRB 221009A to search for signatures of Lorentz violation. We employ the DisCan (dispersion cancellation) method with various information entropies as cost functions, designating the results obtained with Shannon entropy as our representative outcome. This choice is attributed to the parameter-free statistical properties of Shannon entropy, which has demonstrated remarkable stability as we continually refine and enhance our methodology. In the absence of more detailed data and physical context, it provides more stable and reliable results. We constrain the energy scale associated with Lorentz invariance violation. Our results yield 95% confidence level lower limits of $E_{QG,1} > 5.4 \times 10^{19}$ GeV (subluminal) and $E_{QG,1} > 2.7 \times 10^{19}$ GeV (superluminal) for the linear case ($n = 1$), and $E_{QG,2} > 10.0 \times 10^{12}$ GeV (subluminal) and $E_{QG,2} > 2.4 \times 10^{12}$ GeV (superluminal) for the quadratic case ($n = 2$). Subsequently, we incorporate WCDA photons and the Knuth binning method to further optimize and complement our approach while also performing filtering using information entropies. Furthermore, we demonstrate that employing different information entropy measures as cost functions does not alter the order of magnitude of these constraints.

Keywords: Lorentz invariance violation, DisCan method, LHAASO

DOI: 10.1088/1674-1137/adfa01

CSTR: 32044.14.ChinesePhysicsC.49125101

I. INTRODUCTION

Lorentz symmetry is a fundamental principle in modern physics, serving as a cornerstone of both special relativity and quantum field theory. However, despite the high-precision testing of symmetry across various contexts, significant motivation exists to explore potential violations. A key motivation is the quest to resolve a fundamental challenge in modern physics: the reconciliation of General Relativity (GR) with Quantum Field Theory (QFT). While GR and QFT have achieved notable empirical success, they leave crucial questions unanswered, such as the emergence of spacetime singularities in GR. Addressing these issues necessitates a comprehensive quantum theory of gravity. Several Quantum Gravity (QG) models suggest the potential violation of Lorentz symmetry at scales where QG effects become significant, as evidenced by various studies [1–8]. This provides a compelling rationale for investigating Lorentz Invariance Violation (LIV) (for an overview, refer to [9]).

Recent advancements in high-energy astrophysical observations provide extra motivations for testing LIV beyond theoretical conjectures. Notably, the subtle spectral deviations between the Greisen-Zatsepin-Kuzmin (GZK) suppression features and theoretical predictions [10–12], alongside the anomalous attenuation deficit of TeV gamma rays from Active Galactic Nuclei (AGN), termed the TeV gamma-ray crisis [13], serve as pivotal observational probes owing to their acute sensitivity to potential LIV [14]. These astrophysical phenomena serve as pivotal avenues for detecting potential violations of Lorentz symmetry. They offer essential insights into exploring deviations from standard dispersion relations in high-energy contexts. Pioneering work by researchers like collaborations such as MAGIC [15–19] have established increasingly stringent limits on potential Lorentz symmetry violations, particularly in high-energy astrophysical contexts. Our work is inspired by the efforts of the MAGIC collaboration [15], aiming to verify whether similar constraints can be obtained in different source

Received 30 March 2025; Accepted 11 August 2025; Published online 12 August 2025

* Supported by the National Natural Science Foundation of China (12375049) and Key Program of the Natural Science Foundation of Jiangxi Province (20232ACB201008)

† E-mail: shufuwen@ncu.edu.cn

©2025 Chinese Physical Society and the Institute of High Energy Physics of the Chinese Academy of Sciences and the Institute of Modern Physics of the Chinese Academy of Sciences and IOP Publishing Ltd. All rights, including for text and data mining, AI training, and similar technologies, are reserved.

scenarios.

The Dispersion Cancellation (DisCan) method [20], an effective technique for investigating LIV, does not require a pre-specified light curve model, in contrast to the maximum likelihood method. We utilize the comprehensive photon dataset from the Large High Altitude Air Shower Observatory (LHAASO) [21], specifically the Kilometer Square Array (KM2A) and Water Cherenkov Detector Array (WCDA) detector. KM2A is a ground-based particle detector array covering approximately one square kilometer, composed of electromagnetic particle and muon detectors. Its primary strength lies in high-sensitivity detection of gamma and cosmic rays in the energy range from tens of TeV to PeV, enabling effective discrimination between cosmic-ray backgrounds and gamma-ray signals. WCDA comprises three large water pools with a total area of 78,000 m², utilizing Cherenkov light radiation to cover the 100 GeV to tens of TeV energy range. The key advantages of WCDA include its wide field of view, nanosecond-level timing resolution, and all-weather monitoring capability, making it particularly adept at capturing rapid variability in high-energy astrophysical phenomena. This method offers a novel approach to constraining potential Lorentz symmetry breaking. The motivation emanates from the need to probe fundamental physics at energy scales approaching quantum gravity thresholds.

In this study, we focus on analyzing the time-of-flight measurements of photons from GRB 221009A [22], one of the brightest gamma-ray bursts ever detected. We apply the DisCan method in conjunction with various information entropies as cost functions and the Knuth binning method [23] to optimize the original fixed equal-bin distribution, aiming to provide improved constraints on potential LIV. Through the comparison of different information entropies, such as Shannon, Rényi, and Tsallis entropies, we derive effective limits on LIV that are consistent with previous NASA findings [20], indicating that Shannon entropy as a cost function yields higher credibility. More significantly, we extrapolate this approach to long-duration bursts and high-energy regimes, not only with simulated data, thus expanding the application domain of the DisCan method.

The remainder of this paper is structured as follows: Section II presents the theoretical background and methodological approach. Section III details the DisCan method and its implementation. Section IV discusses the results and their implications. Finally, Section V offers our discussions and conclusions.

II. METHODS AND APPROACHES

Quantum gravity theories propose that space-time exhibits quantum fluctuations, which may lead to a non-trivial refractive index that influences the propagation of

particles [24]. Different quantum gravity models suggest that the speed of particle propagation can vary with energy, a phenomenon referred to as LIV.

A fundamental expectation associated with quantum gravity is a modified photon dispersion relation [25]

$$E^2 = p^2 c^2 \left[1 + \sigma \left(\frac{E}{\varepsilon_{QG,n}^{(\sigma)} E_{Pl}} \right)^n \right], \quad (1)$$

where $E_{Pl} \approx 1.22 \times 10^{19}$ GeV is the Planck energy. The parameter $\varepsilon_{QG,n}^{(\sigma)}$ quantifies the LIV energy scale relative to E_{Pl} . Typically, the value of n is 1 or 2, corresponding to first-order or second-order breaking energy scales, respectively. The index $\sigma = \pm 1$ indicates the direction of dispersion modification.

This dispersion relation introduces an energy-dependent photon velocity. In the regime where $E \ll \varepsilon_{QG,n} E_{Pl}$, we can express the relationship as

$$v = c \left[1 + \sigma \frac{n+1}{2} \left(\frac{E}{\varepsilon_{QG,n}^{(\sigma)} E_{Pl}} \right)^n \right]. \quad (2)$$

Photon propagation can exhibit either subluminal or superluminal characteristics, which correspond to $\sigma = -1$ and $\sigma = +1$, respectively. This energy-dependent velocity results in a time of flight (TOF) for a photon with energy E that differs from what would be expected if it traveled at the conventional speed of light [26].

The modified TOF can be mathematically represented as [26]

$$\delta t_{LIV}(E) = -\sigma \frac{n+1}{2H_0} \left(\frac{E}{\varepsilon_{QG,n}^{(\sigma)} E_{Pl}} \right)^n \int_0^z \frac{(1+\zeta)^n d\zeta}{\sqrt{\Omega_M(1+\zeta)^3 + \Omega_\Lambda}}, \quad (3)$$

where z denotes the redshift of the source. The Hubble-Lemaître constant, denoted as H_0 , is taken to be approximately 67.5 km s⁻¹ Mpc⁻¹. The current fraction of matter in the Universe is represented by $\Omega_M = 0.315$, whereas the cosmological constant fraction is $\Omega_\Lambda = 0.685$ [27]. Specifically, for GRB 221009A, which has a redshift of $z = 0.151$ [28], the relevant values are utilized in the expression.

In this study, which also uses the publicly accessible data from LHAASO for an initial exploration, we apply a different approach from Piran's phenomenological average correction constant. Specifically, we utilize the complete time-energy information data of photons detected by KM2A [28] during GRB 221009A and apply the DisCan method to impose observational constraints on the potential Lorentz violation energy scale. The results obtained from our analysis mutually validate the findings of Piran's work.

The DisCan method is an algorithm for detecting quantum gravity dispersion in photons. The algorithm adjusts the arrival times of photons to cancel out the dispersion caused by quantum gravity effects, thereby detecting the energy-dependent time delays. We assume that the energy-dependent time delay is given by [20]

$$t_{\text{obs}} = t_{\text{true}} + \theta_1 \cdot E, \quad (4)$$

where t_{obs} is the observed arrival time, t_{true} denotes the time at which the photon would have arrived had it suffered no quantum gravity time shift [20], θ_1 is the dispersion coefficient when $n = 1$, and E is the photon energy, with the time unit in s and the dispersion coefficient unit in s/TeV . Similarly, we can also assume a quadratic energy-dependent time delay as

$$t_{\text{obs}} = t_{\text{true}} + \theta_2 \cdot E^2, \quad (5)$$

where θ_2 is the dispersion coefficient when $n = 2$, with the dispersion coefficient unit in s/TeV^2 .

For both the first-order and second-order delay cases, we construct a time profile using the adjusted arrival times. Subsequently, we optimize the sharpness of the time profile to determine the best dispersion coefficient θ_i using Shannon, Rényi, and Tsallis entropies.

Based on the given formulas (3)–(5) and numerical values and $\delta t_{\text{LIV}}(E) = t_{\text{obs}} - t_{\text{true}}$, we can derive

$$\varepsilon_{\text{QG},1}^{(\sigma)} \simeq -5.7\sigma/\theta_1 \quad n = 1, \quad (6)$$

$$\varepsilon_{\text{QG},2}^{(\sigma)} \simeq -7.5\sigma/(10^8 \cdot \theta_2) \quad n = 2. \quad (7)$$

Because ε_{QG} is always positive, we can determine σ using the parameter θ_i , thereby determining whether it is superluminal or subluminal.

The advantage of the DisCan method is its applicability to arbitrary dispersion models and its high sensitivity. By adjusting the photon arrival times, the DisCan method can effectively detect the small time delays caused by quantum gravity effects. We investigate time-of-flight constraints on LIV derived from KM2A observations of TeV photons from GRB 221009A, the brightest gamma-ray burst, and appropriately incorporated the low-energy photon data observed by WCDA.

III. ANALYSIS USING DISCAN

The DisCan method is applicable to any dispersion model and can detect small time delays caused by quantum gravity effects. For this study, after constructing the linear dispersion model, we first select a cost

function for the overview of time after binning to optimize the selection of θ_1 and θ_2 and obtain the corresponding LIV parameters $\varepsilon_{\text{QG},1}^{(\sigma)}$ and $\varepsilon_{\text{QG},2}^{(\sigma)}$. Finally, the breaking energy scales for $E_{\text{QG},1}$ and $E_{\text{QG},2}$ are obtained.

The LIV parameters θ_i ($i = 1, 2$) are estimated by maximizing the information content of the reconstructed time profiles using transformed photon arrival times through dispersion relations (4) and (5). We employ three information-theoretic measures as cost functions:

• Shannon entropy

Shannon entropy is defined [29] as

$$H_S = - \sum_n p_n \log p_n, \quad (8)$$

where $p_n \equiv x_n / \sum x_n$ represents the normalized photon count probability [20], with x_n denoting the photon intensity in temporal bins. As the foundational measure of information uncertainty, it achieves maximal sensitivity for peaked distributions. Subsequent entropies also continue to employ these two concepts.

• Rényi entropy

Rényi entropy is given [30] by

$$H_R(\alpha) = \frac{1}{1-\alpha} \log \left(\sum_n p_n^\alpha \right). \quad (9)$$

This generalized entropy reduces to Shannon entropy when $\alpha \rightarrow 1$, with $\alpha > 1$ emphasizing high-probability bins and $\alpha < 1$ enhancing sensitivity to rare events.

• Tsallis entropy

The expression for Tsallis entropy is [31]

$$H_T(q) = \frac{1}{q-1} \left(1 - \sum_n p_n^q \right). \quad (10)$$

It is characterized by the non-extensive parameter $q \neq 1$ and has the same regulatory effect as α . Originally developed for non-equilibrium thermodynamics, this measure demonstrates superior performance in systems with long-range correlations.

When entropy is minimized, the information at the source is most certain, and it is most likely to obtain the true time profile, thereby obtaining the broken parameter.

IV. RESULTS

We utilize the publicly available KM2A observational data from the LHAASO collaboration [28] to investigate the values of the parameters θ_i obtained under first-

and second-order linear models, thereby deriving the corresponding energy scale $E_{QG,n}$ for LIV. Initially, we utilized only the photon time-energy data from KM2A and referenced the 10-s binning provided by LHAASO to maintain the original equal-bin distribution [28]. Subsequently, we incorporated additional photon data from WCDA and replaced the original equal-bin distribution with the Knuth binning method. The Knuth binning method is a type of equal-bin method that employs a piecewise constant density model with equal bin widths. It utilizes the maximum Bayesian posterior probability to directly quantify the likelihood of binning. Its primary advantage is its adaptability to any distribution, including multi-peaked, asymmetric, and complex structures, enabling it to effectively capture complex temporal structures. Notably, this method requires minimal to no prior information [23]. Our approach to handling WCDA photon data also references the methodology of the LHAASO collaboration [22].

Because WCDA photons are initially assumed to have identical energy, with any subsequent variations in energy attributable solely to statistical fluctuations, we posit that these photons do not enhance the clarity of the source reconstruction. Instead, they significantly diminish the influence of KM2A photons. Consequently, subtracting the information entropy generated by WCDA photons following the binning process is considered appropriate. This leads to a natural adoption of a refined approach, wherein the information entropy, originally defined by the combined contributions of KM2A and WCDA photons, is adjusted by subtracting the information entropy derived exclusively from WCDA photons. This adjustment effectively replaces the traditional notion of information entropy with the concept of relative information entropy.

To account for photon energy uncertainties, we apply a Monte Carlo-based blurring technique to the photon energies, assuming Gaussian errors. In our Monte Carlo simulations ($n_{\text{sim}} = 1000$), we model energy measurement uncertainties using asymmetric Gaussian distributions. For each data point i , positive errors follow $\mathcal{N}(\mu = 0, \sigma = \sigma_{+i})$ and negative errors follow $\mathcal{N}(\mu = 0, \sigma = \sigma_{-i})$, where σ_{+i} and σ_{-i} are the observed upper and lower 1σ error bounds, respectively. For each realization, we generate random variates $z \sim \mathcal{N}(0, 1)$ and compute the error term as

$$\delta_i = \begin{cases} \sigma_{+i} \cdot z, & z \geq 0, \\ \sigma_{-i} \cdot |z|, & z < 0. \end{cases}$$

Synthetic energy samples are then generated through the following transformation:

$$E_{\text{sample},i} = \max(0, E_{\text{obs},i} + \delta_i).$$

We construct the histogram distribution of the parameter θ_i . The 95% confidence interval is indicated by a dashed line in the plot.

Figures 1 and 2 show the histogram distributions of the parameters θ_1 and θ_2 obtained from 1000 Monte Carlo samples, with the dashed lines indicating the 95% confidence intervals. We observe that, when using Shannon entropy as the cost function, the resulting parameters θ_i exhibit shorter confidence intervals and higher concentrations in the same order, without the introduction of additional parameters. Therefore, we recommend the results obtained from Shannon entropy as the summary. Nevertheless, the results obtained using Rényi and Tsallis entropies remain significant. They offer insights that complement findings from other entropy measures, such as Shannon entropy. Additionally, as both our linear energy-dependent time delay formulas (4) and (5) and the use of information entropy as a cost function ignore some deeper physical considerations, such as the omission of extragalactic background light (EBL) absorption in the propagation model, source-intrinsic energy-dependent photon emission delays, and other unmodeled systematic uncertainties. Nevertheless, they still hold significance as observable tests for quantum gravity theories and comparative studies with other Lorentz symmetry violations.

Figures 3, 4, and 5 present the histogram of the θ_i distribution obtained after incorporating WCDA photons and applying the Knuth binning method. When employing the Knuth binning method, we directly exclude the scenario where relative Rényi entropy is used as the cost function. Additionally, a comparison is conducted for the parameter (q) in relative Tsallis entropy, revealing that the case with $q = 0.5$ is superior to that with $q = 2$. The physical interpretation of this finding is that our system exhibits significant non-extensivity, indicating that the total entropy of the system is not merely the sum of the entropies of its subsystems—a characteristic notably associated with Rényi entropy. In the analysis of gamma-ray burst (GRB) photon time series, the arrival times of photons may exhibit long-range correlations influenced by quantum gravity effects. Tsallis entropy with $q < 1$ is more adept at capturing such correlations. Moreover, our adoption of relative entropy analysis reveals that the current task necessitates a focus on low-probability, high-value tail information—specifically, the KM2A photon data. This implies that the system may involve complex interactions that conventional extensive entropy measures cannot fully characterize. However, note that the generality of this feature remains unverified. Future work should employ the DisCan method to conduct similar analyses on additional gamma-ray burst sources to validate these findings.

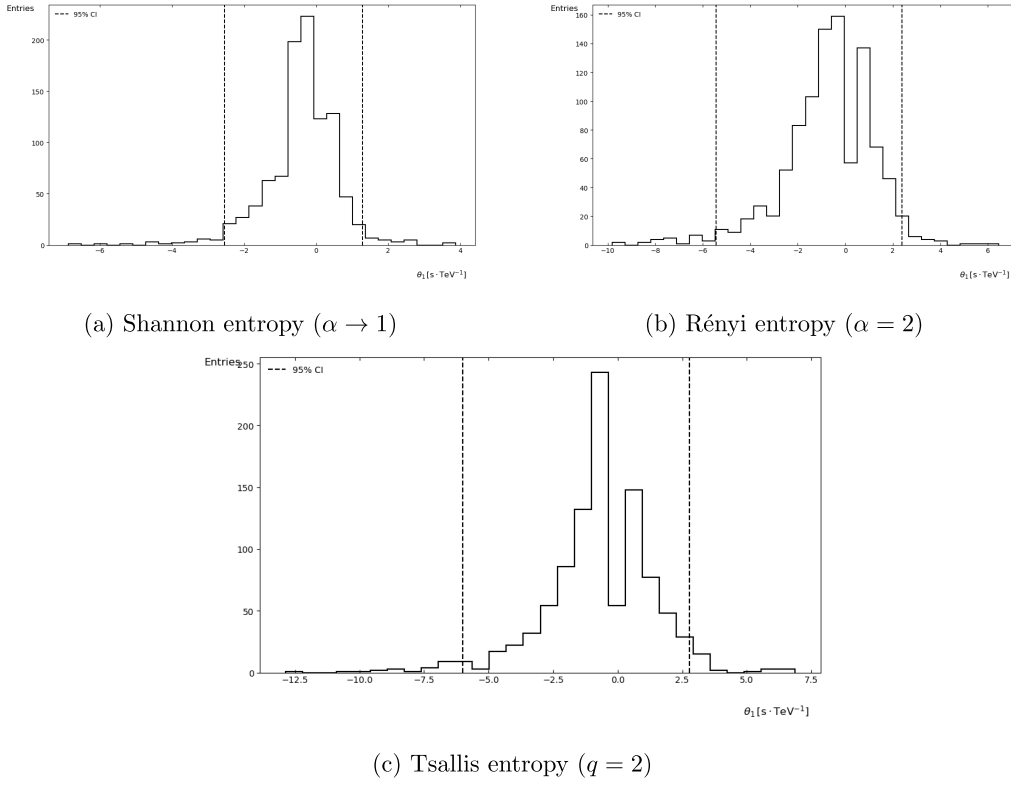


Fig. 1. Probability density distributions of the first-order Lorentz invariance violation parameter θ_1 estimated through (a) Shannon entropy (baseline case), (b) Rényi entropy with $\alpha = 2$, and (c) Tsallis entropy with $q = 2$. Vertical dashed lines indicate 95% confidence intervals. All histograms contain 1,000 Monte Carlo realizations with identical color mapping and axis scaling.

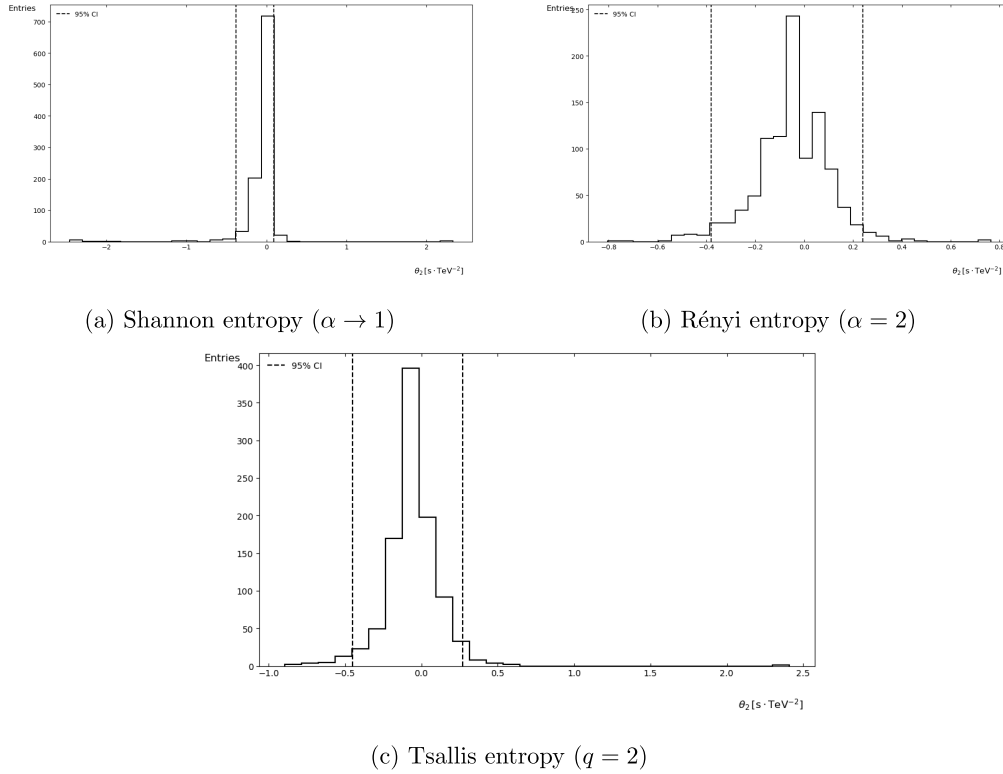


Fig. 2. Probability density distributions of the second-order Lorentz invariance violation parameter θ_2 estimated through (a) Shannon entropy (baseline case), (b) Rényi entropy with $\alpha = 2$, and (c) Tsallis entropy with $q = 2$. Vertical dashed lines indicate 95% confidence intervals. All histograms contain 1,000 Monte Carlo realizations with identical color mapping and axis scaling.

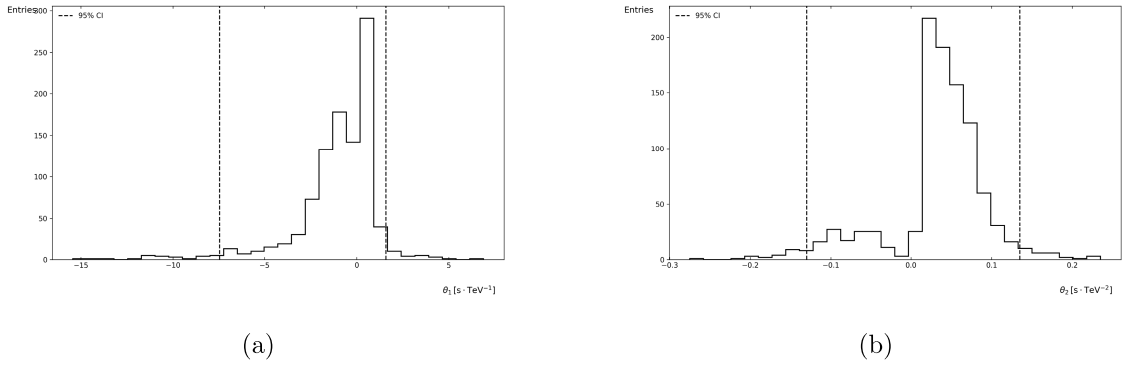


Fig. 3. Distribution histograms of parameters θ_1 and θ_2 derived from the application of Knuth's optimal binning algorithm with relative Shannon entropy as the cost function.

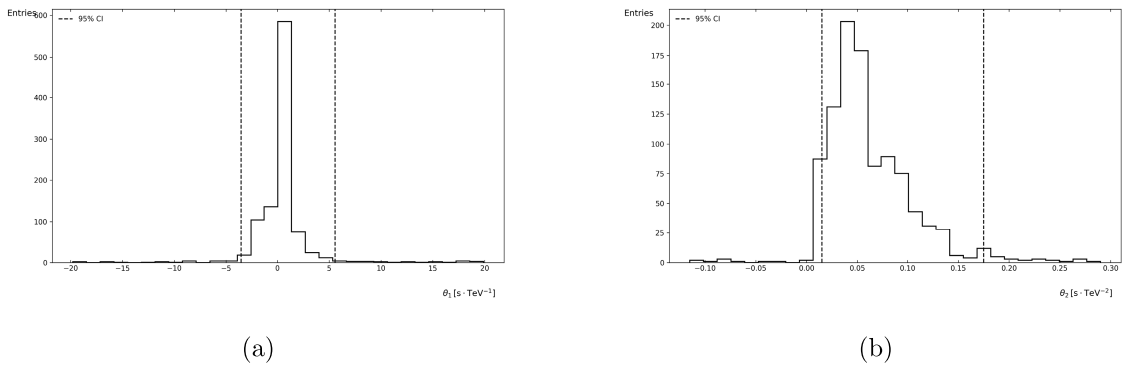


Fig. 4. Distribution histograms of parameters θ_1 and θ_2 derived from the application of Knuth's optimal binning algorithm with relative Tsallis entropy ($q = 2$) as the cost function.

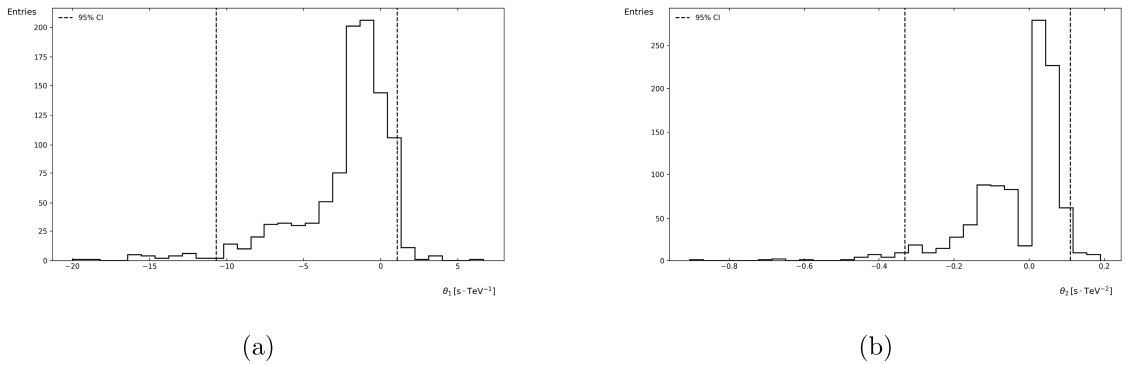


Fig. 5. Distribution histograms of parameters θ_1 and θ_2 derived from the application of Knuth's optimal binning algorithm with relative Tsallis entropy ($q = 0.5$) as the cost function.

Our initial motivation for introducing Tsallis entropy was its non-extensivity, which naturally describes non-local propagation effects. Additionally, when the dispersion relation is non-linear, the non-extensive framework of Tsallis entropy is more easily extended to multi-parameter optimization. This inspires us to consider modifying the dispersion relation and incorporating more quantum gravity spacetime characteristics into the model in future research.

Tables 1, 2, and 3 list the 95% confidence intervals for the parameters θ_i , $\varepsilon_{QG,n}$, and $E_{QG,n}$, where $\sigma = +1$ represents the superluminal case, and $\sigma = -1$ represents the subluminal case. For the parameter θ , regardless of whether it is first-order or second-order, and regardless of the entropy measure used as the cost function, the absolute value of the lower bound is always greater than that of the upper bound. We have obtained conclusions consistent with those of the LHAASO collaboration [22]. This indicates that the distribution is not symmetric but rather biased. An additional feature observed in Figs. 3–5 is that, after we incorporate WCDA photons (which exhibit lower energy contrast compared to KM2A photons)

represents the superluminal case, and $\sigma = -1$ represents the subluminal case. For the parameter θ , regardless of whether it is first-order or second-order, and regardless of the entropy measure used as the cost function, the absolute value of the lower bound is always greater than that of the upper bound. We have obtained conclusions consistent with those of the LHAASO collaboration [22]. This indicates that the distribution is not symmetric but rather biased. An additional feature observed in Figs. 3–5 is that, after we incorporate WCDA photons (which exhibit lower energy contrast compared to KM2A photons)

Table 1. 95% CIs for θ_1 and θ_2 .

	θ_1 (s/TeV)		θ_2 (s/TeV ²)	
	Lower	Upper	Lower	Upper
H_S	-2.545	1.290	-0.380	0.090
$H_R(\alpha = 2)$	-5.435	2.380	-0.380	0.240
$H_T(q = 2)$	-6.007	2.770	-0.450	0.270

Table 2. 95% CIs for $\varepsilon_{QG,1}$ and $\varepsilon_{QG,2}$.

	$\varepsilon_{QG,1}$		$\varepsilon_{QG,2}$ (10 ⁻⁷)	
	$\sigma = +1$	$\sigma = -1$	$\sigma = +1$	$\sigma = -1$
H_S	2.2	4.4	2.0	8.3
$H_R(\alpha = 2)$	1.0	2.4	2.0	3.1
$H_T(q = 2)$	0.95	2.1	1.7	2.8

Table 3. 95% CIs for $E_{QG,1}$ and $E_{QG,2}$.

	$E_{QG,1}$ (10 ¹⁹ GeV)		$E_{QG,2}$ (10 ¹² GeV)	
	$\sigma = +1$	$\sigma = -1$	$\sigma = +1$	$\sigma = -1$
H_S	2.7	5.4	2.4	10.0
$H_R(\alpha = 2)$	1.3	2.9	2.4	3.8
$H_T(q = 2)$	1.2	2.5	2.0	3.4

and apply the Knuth binning method, the photon distribution exhibits a preference for subluminal propagation. This trend contrasts with the results obtained from KM2A data alone.

Table 4 shows that for the relative Tsallis entropy with $q = 2$, in the second-order scenario, both lower and upper limits for the second-order Lorentz violation energy scale are obtained. When employing the Knuth binning method and relative $H_T(q = 2)$ entropy, the following results are derived: in the superluminal case, the lower limit for $E_{QG,1}$ is 2.0×10^{19} GeV; in the subluminal case, the lower limit for $E_{QG,1}$ is 1.2×10^{19} GeV; additionally, in the subluminal case, the lower limit for $E_{QG,2}$ is 5.2×10^{12} GeV and the upper limit is 6.1×10^{13} GeV. These limits are determined based on the 95% confidence interval. The results in Tables 4 and 5 demonstrate that we have further considered the influence of the afterglow of GRB 221009A and the effect of parameter adjustment in Tsallis entropy.

In the process of deriving $E_{QG,n}$ from $\varepsilon_{QG,n}$, we find that, regardless of whether the first-order or second-order linear delay model is used, the subluminal constraint is always stronger than the superluminal one. Specifically,

Table 4. 95% CIs for θ_1 and θ_2 with Knuth's binning method and relative entropy.

	θ_1 (s/TeV)		θ_2 (s/TeV ²)	
	Lower	Upper	Lower	Upper
H_S	-7.476	1.586	-0.130	0.135
$H_T(q = 2)$	-3.556	5.577	0.015	0.175
$H_T(q = 0.5)$	-10.676	1.080	-0.330	0.110

Table 5. 95% CIs for $E_{QG,1}$ and $E_{QG,2}$ with Knuth's binning method and relative entropy.

	$E_{QG,1}$ (10 ¹⁹ GeV)		$E_{QG,2}$ (10 ¹² GeV)	
	$\sigma = +1$	$\sigma = -1$	$\sigma = +1$	$\sigma = -1$
H_S	0.93	4.4	7.0	6.8
$H_T(q = 0.5)$	0.65	6.4	2.8	8.3

the first-order energy scale is on the order of 10^{19} GeV, and the second-order energy scale is on the order of 10^{12} GeV. The constraints obtained using Shannon entropy as the cost function are stricter, indicating that it provides more comprehensive results in the absence of additional physical considerations.

V. DISCUSSIONS AND CONCLUSIONS

In this study, we employed the DisCan method with different information entropy measures to investigate the constraints on LIV parameters using LHAASO's KM2A observational data of GRB 221009A. Similar constraints were obtained using different entropy measures. Specifically, using the DisCan method with Shannon entropy, the 95% confidence level lower limits for the subluminal (superluminal) scenarios were determined to be $E_{QG,1} > 5.4(2.7) \times 10^{19}$ GeV for the linear case ($n = 1$) and $E_{QG,2} > 10.0(2.4) \times 10^{12}$ GeV for the quadratic case ($n = 2$). By using the alternative Rényi entropy with $\alpha = 2$, the lower limits were found to be $E_{QG,1} > 2.9(1.3) \times 10^{19}$ GeV and $E_{QG,2} > 3.8(2.4) \times 10^{12}$ GeV, whereas Tsallis entropy with $q = 2$ produced similar results to Rényi entropy. The Lorentz-violating energy scale obtained in our study is approximately of the same order of magnitude as that derived from the recent work by LHAASO [32]. These results indicate that while the exact choice of entropy measure affects the precise values, the order of magnitude of the LIV energy scale remains consistent. As an optimization and supplement to the initial methods, we incorporated WCDA photons and the Knuth binning method to

1) In some cases, the inferred linear LIV scale $E_{QG,1}$ exceeds the Planck energy $E_{Pl} \approx 1.22 \times 10^{19}$ GeV (similar results also have been observed in previous references [22, 32]). Theoretically, this potentially implies the absence of first-order Lorentz symmetry breaking. However, there are some quantum gravity theories which have energy scales beyond E_{Pl} [33, 34]. In that case, this gives a stringent constraint on the energy scale of the potential first-order Lorentz symmetry breaking. Phenomenologically, these apparent super-Planckian values possibly indicate unmitigated systematic effects. Future multi-messenger observations (such as gamma-ray bursts (GRBs) and active galactic nuclei (AGNs)) could resolve these ambiguities by reducing statistical uncertainties and constraining source-related systematics.

enhance the original approach. This not only makes the results more diverse and engaging but also highlights the differences when various information entropies are employed as cost functions. Additionally, it underscores the further screening effect of the Knuth binning method on information entropy. Our findings indicate that Rényi entropy, being an additive entropy, is less suitable than Tsallis entropy for systems characterized by long-range interactions. Consequently, this insight directs our future research efforts toward a more in-depth investigation of the parameter (q). Note that, currently, our findings do not definitively suggest the existence of long-range interactions in the observed gamma-ray burst spectra. To obtain more definitive signals, we must conduct similar analyses on other events, such as GRB 130427A and GRB 190114C. This aspect of the research will be undertaken in future work.

The derived constraints for the LIV parameters θ_1 and θ_2 , as well as the corresponding energy scales $E_{QG,1}$ and $E_{QG,2}$, reveal a clear preference for subluminal scenarios, with stronger limits in the subluminal regime. Although we only used the KM2A data and lacked more detailed data from the LHAASO collaboration, this conclusion is consistent with theirs [22]. Moreover, the energy scales corresponding to the first-order LIV ($E_{QG,1}$) are on the order of 10^{19} GeV, whereas the second-order LIV scales ($E_{QG,2}$) are on the order of 10^{12} GeV. The use of Shannon entropy as a cost function yields reliable constraints, highlighting its advantage in providing more reliable results when additional physical factors are not incorporated into the model.

Based on Table 1 of [35], the lower limits on the energy scale of LIV are initially constrained by subluminal propagation scenarios. However, as photon energies increase to the TeV range, a significant number of lower limits are derived from superluminal propagation cases. Regarding the gamma-ray burst GRB 221009A, our analysis results are consistent with the conclusions of the LHAASO collaboration [22]. However, the underlying mechanism responsible for superluminal propagation remains unclear. This will be the objective of our next research phase.

The LHAASO collaboration elucidates that the rapid rising and gradual decaying phases of the light curve of the GRB afterglow are particularly sensitive to subluminal LIV effects [22]. This asymmetry occurs because the time-delay signatures induced by subluminal dispersion ($\sigma = -1$) align more prominently with the steep flux variations in the early afterglow phase, thereby yielding tighter constraints compared with superluminal scenarios ($\sigma = +1$), where dispersion effects may be diluted by the smoother temporal evolution. Owing to the rapid rise and

slow decay characteristics of the afterglow, high-energy photons are predominantly concentrated in the early time periods, resulting in a higher accumulation of photons within individual bins. Our method appears to favor an even distribution of photons across each bin, thus preferring a dispersion coefficient θ that shifts the densely packed high-energy photons on the left toward the right. This likely explains why our constraints on subluminal LIV effects are stricter than those on superluminal LIV effects.

Another possible issue is that we have neglected the potential effect of Extragalactic Background Light (EBL) in the present work. However, as found by the LHAASO collaboration in [21], EBL absorption in the present case exerts minimal influence on the light curves of both high-energy and low-energy photons, rendering our methodology largely insensitive to EBL effects.

Note that our methodology is grounded in photon time series counting analysis, which differs from statistical methods that rely on parametric fitting. A promising avenue for future research lies in integrating these two approaches. Significantly, existing literature has accounted for photon emission time effects by employing data from multiple GRBs at different redshifts to conduct statistical joint analyses [36–38], thereby mitigating source-intrinsic effects. Incorporating our method to perform such multiple GRB analysis in the future, to effectively reduce the uncertainty of source effects, would be interesting.

In addition, to validate whether our statistical procedure is robust, we would require to establish that the confidence intervals produced by the method reliably satisfy the desired coverage criteria, as illustrated in [39]. This is another important direction of future work.

In conclusion, our study provides stringent constraints on LIV using the LHAASO observations of GRB 221009A. The results show that the subluminal scenario offers stronger constraints, and Shannon entropy provides the most reliable estimates. However, further refinement of these constraints will require the consideration of additional physical factors, such as EBL absorption and intrinsic energy-dependent emission time effects, as well as the exploration of other quantum gravity models and dispersion relations.

ACKNOWLEDGEMENTS

We extend our gratitude to Yuming Yang for useful discussions, and we particularly thank Xiao-Jun Bi for his insightful discussions and valuable comments. We are grateful to the anonymous referees for their constructive feedback, which greatly improved the quality of this work.

References

- [1] G. Amelino-Camelia, J. R. Ellis, N. E. Mavromatos *et al.*, *Nature* **393**, 763 (1998)
- [2] G. Amelino-Camelia, J. R. Ellis, N. E. Mavromatos *et al.*, *Int. J. Mod. Phys. A* **12**, 607 (1997)
- [3] J. R. Ellis, N. E. Mavromatos, and A. S. Sakharov, *Astropart. Phys.* **20**, 669 (2004)
- [4] R. Gambini and J. Pullin, *Phys. Rev. D* **59**, 124021 (1999)
- [5] S. M. Carroll, J. A. Harvey, V. A. Kostelecky *et al.*, *Phys. Rev. Lett.* **87**, 141601 (2001)
- [6] J. Ellis, N. E. Mavromatos, and D. V. Nanopoulos, *Phys. Rev. D* **61**, 027503 (1999)
- [7] D. Colladay and V. A. Kostelecky, *Phys. Rev. D* **58**(11), 116002 (1998)
- [8] G. Amelino-Camelia, *Nature* **408**(6813), 661 (2000)
- [9] S. Liberati and L. Maccione, *Ann. Rev. Nucl. Part. Sci.* **59**, 245 (2009)
- [10] J. Abraham, P. Abreu, M. Aglietta *et al.*, *Phys. Rev. Lett.* **101**(6), 061101 (2008)
- [11] T. Abu-Zayyad, R. Aida, M. Allen *et al.*, *Astrophys. J. Lett.* **768**(1), L1 (2013)
- [12] R. Abbasi, Y. Abe, T. Abu-Zayyad *et al.*, *Astroparticle Phys.* **151**, 102864 (2023)
- [13] R. J. Protheroe and H. Meyer, *Phys. Lett. B* **493**, 1 (2000)
- [14] K. Toma *et al.*, *Phys. Rev. Lett.* **109**, 241104 (2012)
- [15] J. Albert, E. Aliu, H. Anderhub *et al.*, *Phys. Lett. B* **668**(4), 253 (2008)
- [16] V. A. Acciari, S. Ansoldi, L. A. Antonelli *et al.*, *Phys. Rev. Lett.* **125**(2), 021301 (2020)
- [17] M. L. Ahnen, S. Ansoldi, L. Antonelli *et al.*, *ApJS* **232**(1), 9 (2017)
- [18] J. Albert, E. Aliu, H. Anderhub *et al.*, *Astrophys. J.* **669**(2), 862 (2007)
- [19] T. Zhang, F. W. Shu, Q. W. Tang *et al.*, *Eur. Phys. J. C* **80**(11), 1062 (2020)
- [20] J. D. Scargle, J. P. Norris, and J. Bonnell, *Astrophys. J.* **673**(2), 972 (2008)
- [21] Z. Cao *et al.* (LHAASO Collaboration), *Science* **380**(6652), 1390 (2023)
- [22] Y. M. Yang, X. J. Bi, and P. F. Yin, *JCAP* **2024**(04), 060 (2024)
- [23] K. H. Knuth, *Digital Signal Processing* **95**, 102581 (2019)
- [24] J. Ellis, N. Mavromatos, and D. Nanopoulos, *Phys. Lett. B* **665**(5), 412 (2008)
- [25] T. Piran and D. D. Ofengeim, *Phys. Rev. D* **109**(8), L081501 (2024)
- [26] U. Jacob and T. Piran, *JCAP* **2008**(01), 031 (2008)
- [27] N. Aghanim, Y. Akrami, M. Ashdown *et al.*, *Astronomy & Astrophysics* **641**, A6 (2020)
- [28] Z. Cao *et al.* (LHAASO Collaboration), *Science Advances* **9**(46), 2778 (2023)
- [29] C. E. Shannon, *Bell System Technical Journal* **27**(3), 379 (1948)
- [30] A. Rényi, On measures of entropy and information, in *Proceedings of the fourth Berkeley symposium on mathematical statistics and probability, volume 1: contributions to the theory of statistics*, vol. 4. University of California Press, 1961, pp. 547–562
- [31] C. Tsallis, *Journal of Statistical Physics* **52**, 479 (1988)
- [32] Z. Cao, F. Aharonian, Axikegu *et al.*, *Phys. Rev. Lett.* **133**(7), 071501 (2024)
- [33] D. J. Gross and P. F. Mende, *Nucl. Phys. B* **303**(3), 407 (1988)
- [34] D. Amati, M. Ciafaloni, and G. Veneziano, *Phys. Lett. B* **197**(1-2), 81 (1987)
- [35] J. J. Wei and X. F. Wu, Tests of lorentz invariance, in *Handbook of X-ray and Gamma-ray Astrophysics*. Springer, 2022, pp. 1–30
- [36] J. Ellis, N. E. Mavromatos, D. V. Nanopoulos *et al.*, *Astroparticle Physics* **25**(6), 402 (2006)
- [37] J. Ellis, R. Konoplich, N. E. Mavromatos *et al.*, *Phys. Rev. D* **99**(8), 083009 (2019)
- [38] H. Song and B. Q. Ma, *Astrophys. J.* **983**(1), 9 (2025)
- [39] V. Vasileiou, A. Jacholkowska, F. Piron *et al.*, *Phys. Rev. D—Particles, Fields, Gravitation, and Cosmology* **87**(12), 122001 (2013)